The effect of different ligand substituents on the chemistry of a zinc–pyrazole anion host†

Jonathan Day, Katie E. R. Marriott, Colin A. Kilner and Malcolm A. Halcrow*

Received (in Montpellier, France) 18th August 2009, Accepted 17th September 2009
First published as an Advance Article on the web 26th October 2009
DOI: 10.1039/b9nj00412b

The influence of the pyrazole ligand on the previously reported anion host $[ZnCl(Hpz^{tBu})_3]^+$ (Hpz^{tBu} = 5-*tert*-butylpyrazole) has been investigated. Reaction of $ZnCl_2$ with 3 equiv. of 3{5}-cyclohexylpyrazole (Hpz^{Cy}) or 3{5}-phenylpyrazole (Hpz^{Ph}) affords $[ZnCl(Hpz^R)_3]Cl$ (R = Cy or Ph), both of which undergo decomposition to $[ZnCl_2(Hpz^R)_2]$ upon recrystallisation. A similar reaction using 3{5}-(thien-2-yl)pyrazole (Hpz^{Tn}) affords $[ZnCl_2(Hpz^{Tn})_2]$ only. The salts $[ZnCl(Hpz^{Ph})_3]BF_4$, $[ZnCl(Hpz^{Cy})_3]X$ (X^- = NO_3^-, ClO_4^-, $CF_3SO_3^-$ or $\frac{1}{2}SO_4^{2-}$) and $[ZnBr(Hpz^{Cy})_3]NO_3{\cdot}H_2O$ have been isolated, by performing the above reactions in the presence of 1 equiv. of AgX. The cations in $[ZnCl(Hpz^{Cy})_3]NO_3$ associate into a dimeric capsule encapsulating two nitrate anions. In contrast, $[ZnBr(Hpz^{Cy})_3]NO_3{\cdot}H_2O$ contains hydrogen-bonded $[NO_3{\cdot}H_2O]_n^{n-}$ chains enclosed within channels formed by the complex cations, while $[ZnCl(Hpz^{Cy})_3]ClO_4$ forms a different hydrogen-bonded dimer with the anions occupying two shallow cavities in its surface. These data imply that anion binding by $[ZnCl(Hpz^R)_3]^+$ depends strongly on the steric and inductive properties of the pyrazole 'R' substituents.

Introduction

The continuing interest in anion coordination chemistry[1–5] has been promoted by its relevance to biochemistry and medicine.[6,7] Metal complexes are an important class of anion hosts, in which the metal ion can impart various properties to the system.[2–4,8–10] As well as playing a structural role in maintaining the shape of the anion-binding cavity, the metal ion usually provides a positive charge to the anion receptor that promotes guest binding on Coulombic grounds. In more specific examples the metal ion can itself form part of the anion-binding site by accepting coordinative bonds from the guest,[10] or it can serve as an electrochemical, photometric or fluorescent reporter group in an anion sensor.[2] In a related application, organic ligands designed to coordinate cations and anions simultaneously can serve as extractants for metal salts in liquid–liquid extraction processes.[11]

We and others have described anion hosts based on the $[L_nM(Hpz)_3]^+$ motif, where $[L_nM]^+$ is a transition metal fragment and Hpz is pyrazole or a substituted derivative of it (Scheme 1).[9] While several anion complexes based on this motif have been crystallographically characterised,[12–20] two systems have been studied particularly thoroughly. First is $[ZnCl(Hpz^{tBu})_3]^+$ (Hpz^{tBu} = 5-*tert*-butyl-1*H*-pyrazole), where the three pyrazole NH groups and *tert*-butyl substituents occupy one face of the coordination tetrahedron, forming a bowl-shaped cavity.[14–16] Inorganic anions smaller than PF_6^- form crystalline 1 : 1 adducts with this cation, in which the anions are bound within the cavity by three N–H···X hydrogen bonds (Scheme 1A).[14,15] Larger anions such as PF_6^- and $[Co(C_2B_9H_{11})_2]^-$ are too big for the cavity and instead form 2 : 2 adducts with the complex, which dimerises through intermolecular N–H···Cl hydrogen bonding (Scheme 1B and C).[15,16] Rotation of one or two of the pyrazole groups at each zinc centre about their Zn–N bonds enlarges the cavities, allowing them to bind the larger anions.

Second, Pérez *et al.* have studied a series of octahedral compounds including $[M(CO)_3(HPz^R)_3]^+$ (M = Mn or Re) and $[Mo(\eta^3\text{-}C_3H_5)(CO)_2(HPz^R)_3]^+$ (HPz^R = Hpz^{tBu}, 3,5-dimethyl-1*H*-pyrazole {Hpz′}, 5-phenyl-1*H*-pyrazole {Hpz^{Ph}} or another 1*H*-pyrazole derivative).[18–20] Where available, crystal structures imply that guest anions associate with only two of the three N–H donors at the complex cation (Scheme 1D). This may be a consequence of the small cavity afforded by three pyrazole groups linked by N–M–N angles of ~90° at an octahedral metal ion, which requires severe structural distortions to bind even small guests. In contrast, the pyrazole rings in tetrahedral $[ZnCl(Hpz^{tBu})_3]^+$ are separated by a N–Zn–N angle of *ca.* 109.5°, which affords a larger three-fold cavity that can bind the smaller inorganic anions without any large structural changes (Scheme 1A). In solution, $[ZnCl(Hpz^{tBu})_3]^+$ and $[Re(CO)_3(Hpz^R)_3]^+$ behave as typical anion hosts[21] in that their affinities for different anions depend predominantly on the hydrogen-bond acceptor capability of the guests.[15,18,19] Accurate anion-binding constants were measured for the organometallic receptors, which fall in the range 2×10^1–6×10^3 $dm^3\ mol^{-1}$ in CD_3CN.[18]

School of Chemistry, University of Leeds, Woodhouse Lane, Leeds, UK LS2 9JT. E-mail: M.A.Halcrow@leeds.ac.uk; Fax: +44 (0)113 343 6565; Tel: +44 (0)113 343 6506

† Electronic supplementary information (ESI) available: Additional crystallographic figures and tables for the compounds in this work. CCDC reference numbers 744620–744626. For ESI and crystallographic data in CIF or other electronic format see DOI: 10.1039/b9nj00412b

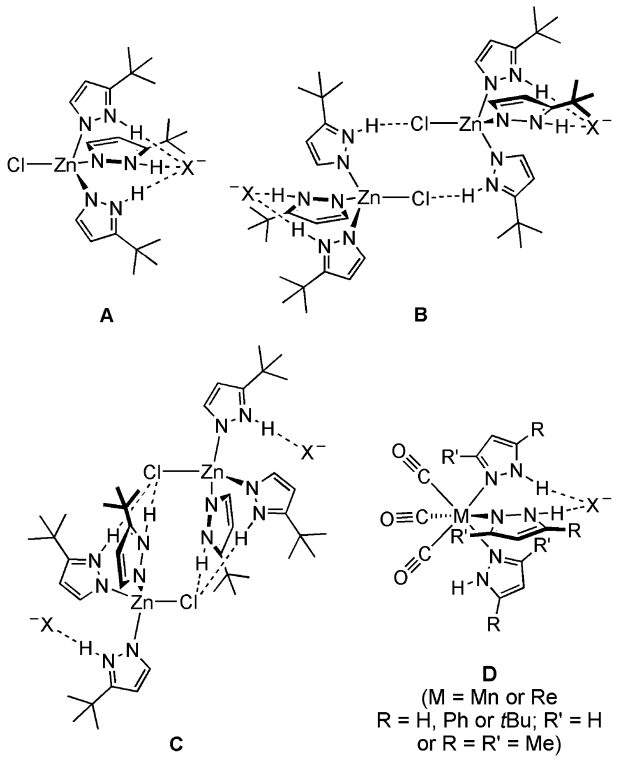

Scheme 1 Two previously reported metal–pyrazole anion hosts, and their modes of guest binding. A, B and C: structures adopted by $[ZnCl(Hpz'^{Bu})_3]^+$ in the presence of differently sized guests X^-. D: one type of organometallic anion host.

Anion-binding constants in solution for $[Re(CO)_3(Hpz^R)_3]^+$ depend significantly on the pyrazole used. For example, the binding constants for Br^- by this receptor in CD_3CN follow the trend in Hpz^R:[18,19]

$$Hpz' > Hpz^{Ph} > Hpz'^{Bu} \approx \text{pyrazole} > \text{indazole}$$

This presumably reflects a combination of steric and electronic factors. Crystal structures of $[Re(CO)_3(Hpz^R)_3]X$ salts with different pyrazole substituents show only small differences in their modes of anion binding (Scheme 1D), however, although more nucleophilic anions can displace pyrazole groups from the metal centre leading to structurally isomeric products $[ReX(CO)_3(Hpz^R)_2]\cdot Hpz^R$.[18,19] To similarly determine the influence of pyrazole substituents on $[ZnCl(Hpz^R)_3]^+$, we now describe a study of three such compounds with different 1*H*-pyrazole ligands Hpz^R (R = cyclohexyl {Cy}, phenyl {Ph} and thien-2-yl {Tn}).

Results and discussion

Reaction of zinc(II) halides with Hpz^R

Reaction of $ZnCl_2$ with 3 equiv. of Hpz^{Cy} or Hpz^{Ph} in MeOH affords a colourless solution, which gives an oily residue upon evaporation to dryness. Crystallisation of the residue from dichloromethane–pentane affords colourless crystalline solids $[ZnCl(Hpz^R)_3]Cl$ (R = Cy or Ph), with the Hpz^{Cy} complex crystallising as a monohydrate. However, recrystallisation of both these complexes from chloroform–diethyl ether led to their partial decomposition, giving a mixture of the starting compounds and the new products $[ZnCl_2(Hpz^R)_2]$. When R = Ph, these two compounds could be isolated separately in pure form by crystallisation under the appropriate conditions. When R = Cy the compounds always co-crystallised, but small amounts of crystalline $[ZnCl_2(Hpz^{Cy})_2]$ were separated manually from powder $[ZnCl(Hpz^{Cy})_3]Cl\cdot H_2O$ for micro-analysis. Treatment of $ZnCl_2$ with 2 or 3 equiv. of Hpz^{Tn} under the same conditions gave $[ZnCl_2(Hpz^{Tn})_2]$ only.

A crystal structure analysis of $[ZnCl(Hpz^{Ph})_3]Cl$ confirmed that it adopts the expected connectivity (Scheme 1A). The complex cation contains a tetrahedral zinc centre, with a non-coordinated chloride ion bound in a pocket formed by the Hpz^{Ph} ligands through three N–H···Cl hydrogen bonds (Fig. 1). The bond lengths and angles about the zinc centre form a more regular tetrahedral coordination geometry compared to $[ZnCl(Hpz'^{Bu})_3]Cl$ (Table 1).[14,15] The weak steric influence of the ligand phenyl substituents on the bound chloride guest is illustrated by the two phenyl rings C(8)–C(13) and C(19)–C(24) in Fig. 1, which are both oriented almost edge-on to the bound anion. The closest C–H···Cl contact between Cl(36) and these phenyl groups is 3.0 Å, outside the sum of the covalent radii of a H and a Cl atom.[22]

Crystal structures of all three $[ZnCl_2(Hpz^R)_2]$ complexes were obtained (R = Cy, Ph and Tn). Although they are not isostructural, each compound crystallises as a hydrogen-bonded dimer, linked by two pairs of N–H···Cl hydrogen bonds (Fig. 2 and ESI†). The chloride ligand not involved in the dimerisation interaction accepts a short C–H···Cl interaction from a chloroform molecule in the solvate $[ZnCl_2(Hpz^{Ph})_2]\cdot CHCl_3$ (Fig. 2). In $[ZnCl_2(Hpz^{Cy})_2]$ and $[ZnCl_2(Hpz^{Tn})_2]$, which are both unsolvated, there is a longer but still significant contact between this Cl atom and a pyrazole *H*4 atom from a neighbouring molecule (ESI†). Interestingly, although there are several other known complexes of the type $[ZnY_2(Hpz^R)_2]$ (Y^- = halide),[23,24] the

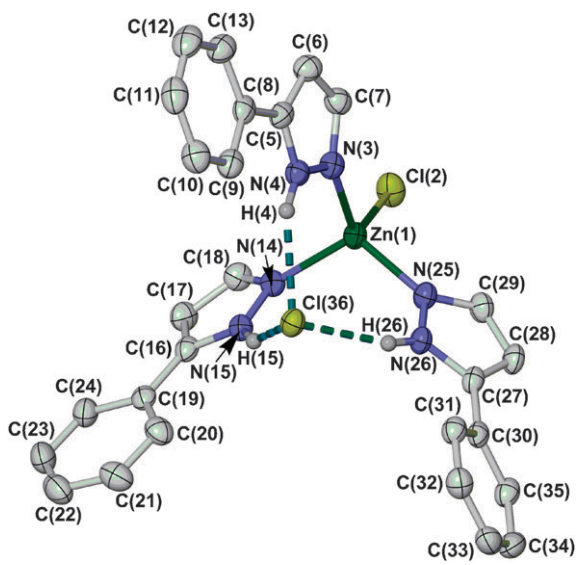

Fig. 1 View of the asymmetric unit of $[ZnCl(Hpz^{Ph})_3]Cl$. All H atoms not involved in hydrogen bonding have been omitted for clarity, and displacement ellipsoids are at the 50% probability level.

Table 1 Selected bond lengths and angles in the crystal structure of $[ZnCl(Hpz^{Ph})_2]Cl$ (Å, °)

Zn(1)–Cl(2)	2.2286(6)	Zn(1)–N(14)	2.0279(15)
Zn(1)–N(3)	2.0169(16)	Zn(1)–N(25)	2.0187(16)
Cl(2)–Zn(1)–N(3)	108.37(5)	N(3)–Zn(1)–N(14)	107.21(6)
Cl(2)–Zn(1)–N(14)	107.85(5)	N(3)–Zn(1)–N(25)	114.65(6)
Cl(2)–Zn(1)–N(25)	106.75(5)	N(14)–Zn(1)–N(25)	111.79(7)

hydrogen-bonded dimer structure adopted by these three compounds has only been observed in one previous example.[24] The coordination geometries about the zinc centres in the three compounds are somewhat flattened (Table 2 and ESI†). The origin of this distortion is unclear, since it is the compound with the bulkiest pyrazole substituents $[ZnCl_2(Hpz^{Cy})_2]$ that exhibits the least distorted coordination geometry (ESI†).

These results contrast with the chemistry of $[ZnCl(Hpz^{tBu})_3]Cl$, which is recrystallised intact from organic solvents. Clearly, the $[ZnCl(Hpz^{R})_3]^+$ cation is stabilised against nucleophilic attack by free Cl^- when R = *t*Bu, compared to when R = Cy, Ph or Tn. This probably reflects a combination of steric factors, where the larger *t*Bu substituents shield the zinc ion from attack; and, the relative basicities of these four monodentate pyrazoles. It is reasonable that the most electron-rich pyrazole ligand in this series, Hpz^{tBu}, should be the most difficult to substitute by other nucleophiles. Consistent with this suggestion, $[ZnBr(Hpz^{Cy})_3]Br$ (prepared from $ZnBr_2$ + 3 equiv. HPz^{Cy} as before), containing the less nucleophilic bromide ion, is stable to decomposition in solution.

Complexes of $[ZnY(Hpz^{R})_3]^+$ (Y^- = Cl^- or Br^-) with other anions

A general route to complexes of $[ZnY(Hpz^{R})_3]X$ with different X^- anions is to react $[ZnY(Hpz^{R})_3]Y$ with 1 equiv. of AgX.[14–16] While we investigated several such reactions using all three of the substituted pyrazoles listed above, the high solubility of many of the products made isolating them as pure solids a challenge. The following compounds were obtained in pure form: $[ZnCl(Hpz^{Ph})_3]BF_4$, $[ZnCl(Hpz^{Cy})_3]X$ (X = NO_3^-, ClO_4^-, $CF_3SO_3^-$ and $\frac{1}{2}SO_4^{2-}$) and $[ZnBr(Hpz^{Cy})_3]NO_3{\cdot}H_2O$, three of which were crystallographically characterised.

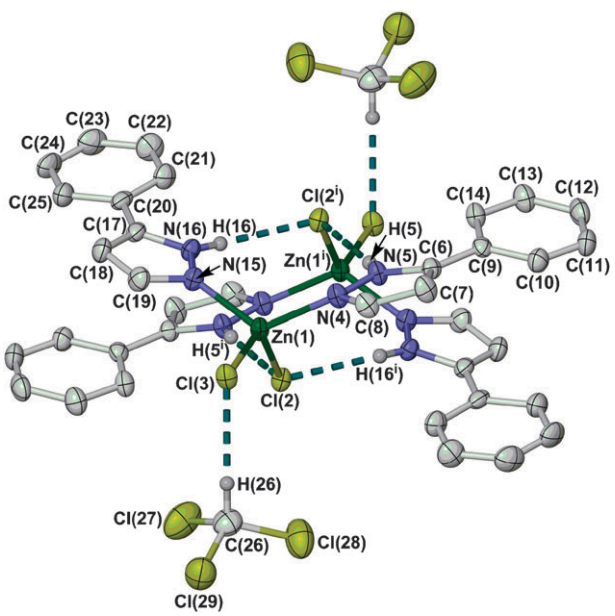

Fig. 2 View of the hydrogen-bonded dimer in the crystal structure of $[ZnCl_2(Hpz^{Ph})_2]{\cdot}CHCl_3$. All H atoms not involved in hydrogen bonding have been omitted for clarity, and displacement ellipsoids are at the 50% probability level. Symmetry code: (i) $1-x$, $1-y$, $1-z$.

Table 2 Selected bond lengths and angles in the crystal structure of $[ZnCl_2(Hpz^{Ph})_2]{\cdot}CHCl_3$ (Å, °). Comparable data for $[ZnCl_2(Hpz^{Tn})_2]$ and $[ZnCl_2(Hpz^{Cy})_2]$ are given in the ESI†

Zn(1)–Cl(2)	2.3189(6)	Zn(1)–N(4)	2.0355(17)
Zn(1)–Cl(3)	2.2470(5)	Zn(1)–N(15)	2.0105(17)
Cl(2)–Zn(1)–Cl(3)	119.86(2)	Cl(3)–Zn(1)–N(4)	106.80(5)
Cl(2)–Zn(1)–N(4)	101.94(5)	Cl(3)–Zn(1)–N(15)	104.38(5)
Cl(2)–Zn(1)–N(15)	103.06(5)	N(4)–Zn(1)–N(15)	121.96(7)

The structures of the two nitrate salts $[ZnY(Hpz^{Cy})_3]NO_3$ (Y^- = Cl^- and Br^-) are notable, in being different from each other and from $[ZnCl(Hpz^{tBu})_3]NO_3$, which adopts the connectivity in Scheme 1A.[15] Both the Hpz^{Cy} complexes contain (approximately) tetrahedral $[ZnY(Hpz^{Cy})_3]^+$ cations with in-cavity nitrate anions (Fig. 3 and Table 3). However, the larger cavities afforded by the cyclohexyl, rather than *tert*-butyl, pyrazole substituents can accommodate additional guest species in addition to a nitrate ion, which manifests itself in different ways in the two structures. The molecules in $[ZnCl(Hpz^{Cy})_3]NO_3$ associate into centrosymmetric, dimeric capsules encapsulating two nitrate guests, with each cation donating two N–H···O hydrogen bonds to one anion and one hydrogen bond to the other (Fig. 3 and Fig. 4). As well as placing both anions in the cavities of both cations, the capsule is formed by interdigitation of the cyclohexyl groups from each half of the supramolecule. Both features are evidence of a more open bowl-shaped cavity in $[ZnCl(Hpz^{Cy})_3]^+$, compared to $[ZnCl(Hpz^{tBu})_3]^+$.[15] The capsule has approximate internal dimensions of 3.9 × 5.9 × 6.9 Å, although there are several openings in its walls (Fig. 4). The two coplanar nitrate guests are separated by 3.155(6) Å, slightly greater than the sum of their van der Waals radii (Fig. 3 and Fig. 4).

The complex molecule in $[ZnBr(Hpz^{Cy})_3]NO_3{\cdot}H_2O$ has crystallographic *m* symmetry, with the mirror plane bisecting the cation, the nitrate ion and water molecule (Fig. 3 and Table 3). In contrast to its chloro analogue, the bowl-shaped cavities in $[ZnBr(Hpz^{Cy})_3]NO_3$ are occupied by the molecule of water, as well as by the nitrate ion. The cation donates two N–H···O hydrogen bonds to the water molecule and one to the nitrate ion, while the water and nitrate are themselves linked by two O–H···O hydrogen bonds (Fig. 3). The latter interactions associate the guest species into polymeric $[NO_3{\cdot}H_2O]_n^{n-}$ zig-zag chains, lying within channels formed by the complex cations (Fig. 5). The channels contain cavities of approximate internal dimensions 4.5 × 5.0 Å, separated by constrictions of 1.9 × 3.6 Å.

The crystal structure of $[ZnCl(Hpz^{Cy})_3]ClO_4$ is different again from the two nitrate compounds, in that the cations associate into dimers through N–H···Cl hydrogen bonding (Scheme 1B; Fig. 6, ESI†). This dimerisation is probably sterically driven, by the binding of larger anions in the host

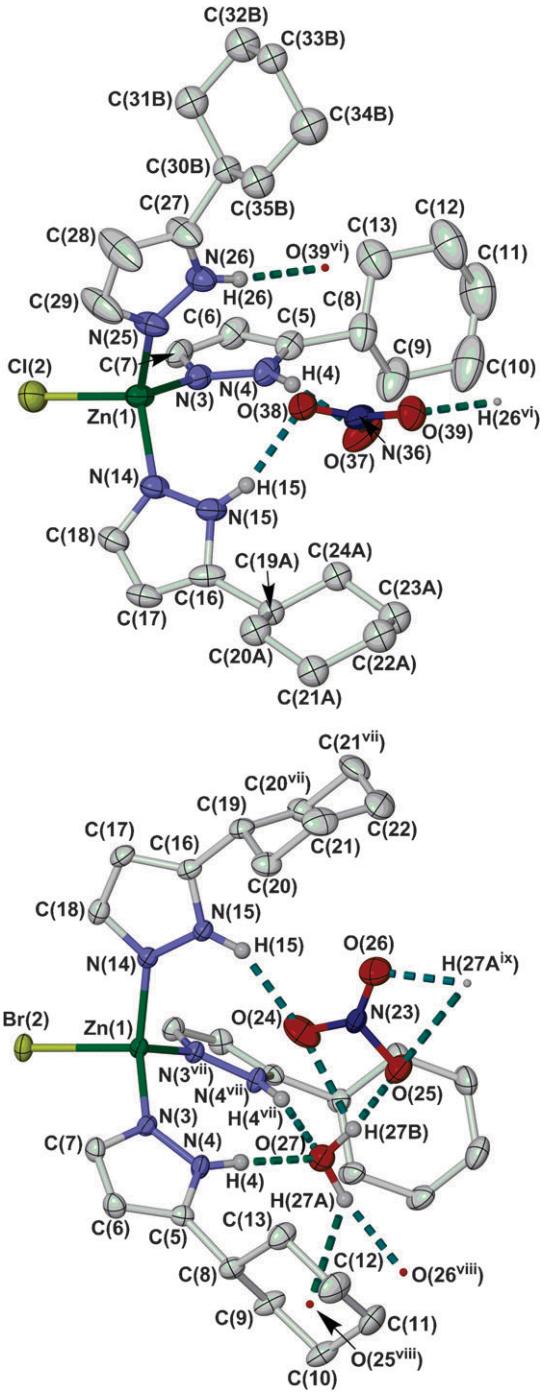

Fig. 3 Views of the formula units in the crystal structures of $[ZnCl(Hpz^{Cy})_3]NO_3$ (top) and $[ZnBr(Hpz^{Cy})_3]NO_3{\cdot}H_2O$ (bottom). All H atoms not involved in hydrogen bonding have been omitted for clarity, and displacement ellipsoids are at the 50% probability level. Only one orientation of the disordered cyclohexyl groups in $[ZnCl(Hpz^{Cy})_3]NO_3$ is shown. Symmetry codes: (vi) $1-x, -y, -z$; (vii) $x, -y+\frac{1}{2}, z$; (viii) $\frac{1}{2}+x, \frac{1}{2}-y, \frac{3}{4}-z$.

cavity. Any steric clashes between the host and guest are relieved by rotation of one pyrazole ring on each zinc centre about its Zn–N bond, so that it presents the face of its five-membered ring to the bowl-shaped cavity rather than its N–H group. The same dimeric structure is exhibited by

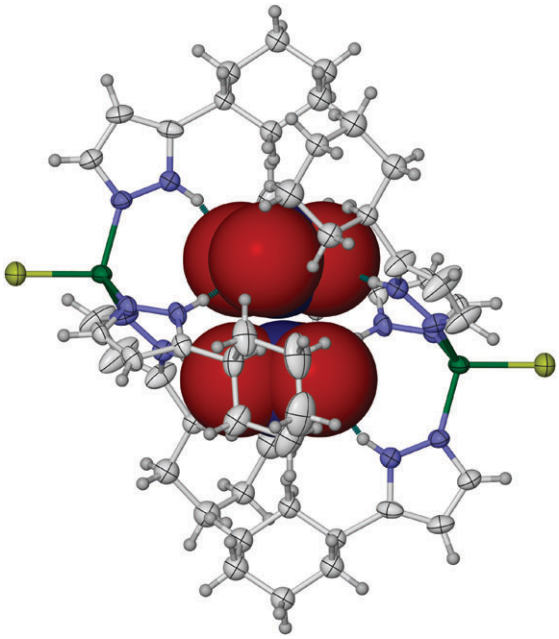

Fig. 4 View of the hydrogen-bonded dimer in $[ZnCl(Hpz^{Cy})_3]NO_3$, showing the pair of nitrate ions (space-filling) encapsulated by two $[ZnCl(Hpz^{Cy})_3]^+$ cations (50% displacement ellipsoids). Only one orientation of the disordered cyclohexyl groups in the structure is shown.

Table 3 Selected bond lengths and angles in the crystal structures of $[ZnCl(Hpz^{Cy})_3]NO_3$ and $[ZnBr(Hpz^{Cy})_3]NO_3{\cdot}H_2O$ (Å, °). Symmetry code: (vii) $x, -y+\frac{1}{2}, z$

$[ZnCl(Hpz^{Cy})_3]NO_3$		$[ZnBr(Hpz^{Cy})_3]NO_3{\cdot}H_2O$	
Zn(1)–Cl(2)	2.2493(7)	Zn(1)–Br(2)	2.4276(5)
Zn(1)–N(3)	2.020(2)	Zn(1)–N(3)	2.0381(19)
Zn(1)–N(14)	2.0229(19)	Zn(1)–N(14)	2.060(3)
Zn(1)–N(25)	2.034(2)	—	—
Cl(2)–Zn(1)–N(3)	108.52(6)	Br(2)–Zn(1)–N(3)	105.49(5)
Cl(2)–Zn(1)–N(14)	105.17(6)	Br(2)–Zn(1)–N(14)	102.82(7)
Cl(2)–Zn(1)–N(25)	108.92(7)	—	—
N(3)–Zn(1)–N(14)	113.61(8)	N(3)–Zn(1)–N(14)	112.28(6)
N(3)–Zn(1)–N(25)	109.70(8)	—	—
N(14)–Zn(1)–N(25)	110.72(8)	N(3)–Zn(1)–$N(3^{vii})$	116.94(10)

$[ZnCl(Hpz^{tBu})_3]PF_6$, but not by $[ZnCl(Hpz^{tBu})_3]ClO_4$ which adopts a mononuclear structure in the crystal (Scheme 1A).[15] However, since the radius of the ClO_4^- ion is only 5% smaller than the PF_6^- ion,[25] we propose that the ClO_4^- guest must be around the maximum size that can be accommodated by a $[ZnCl(Hpz^R)_3]^+$ host (Scheme 1A) without distorting itself.

In the light of these results, the synthesis of $[ZnY(Hpz^{Cy})_3]_2SO_4$ (Y^- = Cl^- or Br^-) was pursued, which could contain a sulfate ion inside a $[ZnY(Hpz^{Cy})_3]_2^{2+}$ capsule. A highly soluble solid $[ZnCl(Hpz^{Cy})_3]_2SO_4$ was isolated from such a reaction, but single crystals of this product could not be obtained.

The electrospray (ES) mass spectra of $[ZnCl_2(Hpz^R)_2]$ (R = Ph, Tn) and of $[ZnCl(Hpz^{Ph})_3]X$ (X^- = Cl^- and BF_4^-) all show predominant mass peaks corresponding to $[^{64}Zn(Hpz^R)_2]^+$ (R = Ph, m/z = 352; R = Tn, m/z = 364). In contrast, the $[ZnCl(Hpz^{Cy})_3]X$ (X^- = Cl^-, NO_3^-, ClO_4^-

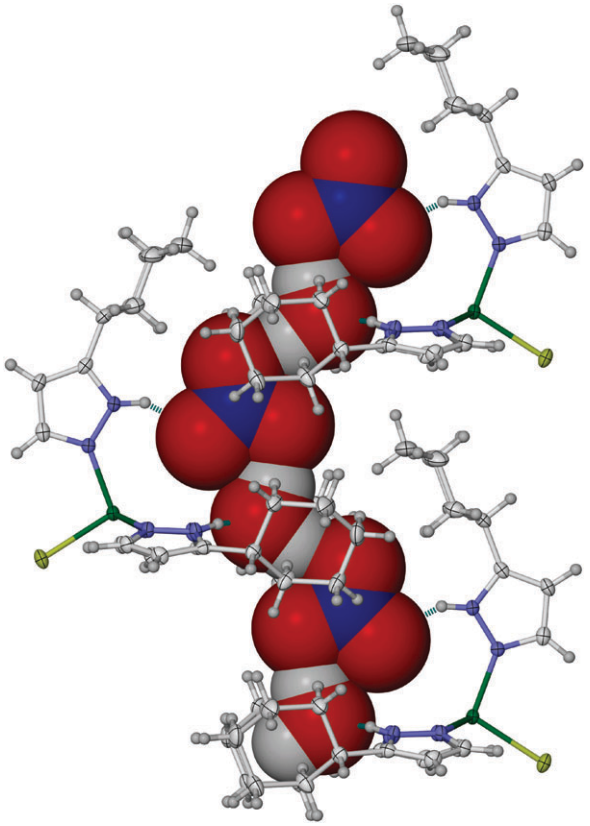

Fig. 5 Partial packing diagram of $[ZnBr(Hpz^{Cy})_3]NO_3{\cdot}H_2O$, showing the $[NO_3{\cdot}H_2O]_n^{n-}$ chains (space-filling) within channels formed by the $[ZnBr(Hpz^{Cy})_3]^+$ cations (50% displacement ellipsoids). The view is approximately along the crystallographic (010) plane, with *c* vertical.

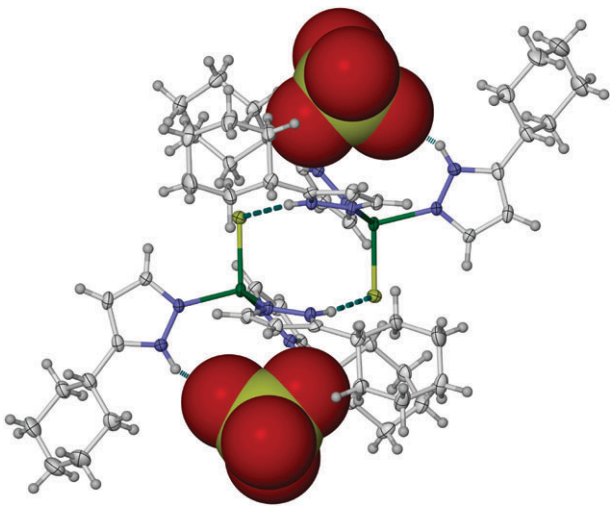

Fig. 6 View of the hydrogen-bonded dimer in $[ZnCl(Hpz^{Cy})_3]ClO_4$, showing the pair of perchlorate ions (space-filling) lying in the bowl-shaped cavities of two $[ZnCl(Hpz^{Cy})_3]^+$ cations (50% displacement ellipsoids).

and $\frac{1}{2}SO_4^{2-}$) and $[ZnBr(Hpz^{Cy})_3]NO_3{\cdot}H_2O$, all exhibit a strong peak for the intact cation $[^{64}ZnY(Hpz^{Cy})_3]^+$ ($Y^- = {}^{35}Cl^-$, m/z = 549; $Y^- = {}^{79}Br^-$, m/z = 593). This is in agreement with our earlier observations about the higher stability of $[ZnCl(Hpz^{Cy})_3]^+$ when R = Cy, compared to the two aryl-substituted pyrazole complexes. There is no peak corresponding to substitution of the Y^- ligand by X^- in any of the $[ZnY(Hpz^{Cy})_3]X$ mass spectra, although some spectra show peaks assignable to $[Zn(O_2CH)(Hpz^{Cy})_3]^+$ and related species from the formate ion present in the ES carrier solution.

The ^1H and ^{13}C NMR spectra of all the compounds in $CDCl_3$ show peaks from a single Hpz^R environment. ^{13}C NMR spectra can indicate the solution stability of pyrazole complexes, since the pyrazole *C*3 and *C*5 peaks are often broadened in free pyrazoles owing to a tautomeric equilibrium[26] that is suppressed when the pyrazole is metal-coordinated.[15] By this measure, all the compounds in this work except the two $[ZnY(Hpz^{Cy})_3]Y$ complexes ($Y^- = Cl^-$ and Br^-) undergo significant solvolysis in $CDCl_3$ since their pyrazole *C*3 and *C*5 NMR peaks were very broad, often to the point of being unobservable. This contrasts with $[ZnCl(Hpz^{tBu})_3]X$ salts, which are all stable in $CDCl_3$ by this criterion in the absence of a large excess of X^- anion.[15]

Conclusions

We have previously shown that $[ZnCl(Hpz^{tBu})_3]^+$ acts as a cavitand host towards a variety of inorganic anions, ranging from Cl^- to $[Co(C_2B_9H_{11})_2]^-$.[14–16] The geometry of the host–guest interaction depends on the size of the guest anion, with large guests causing the compound to lose its (approximate) C_3 symmetry. This leads to dimerisation of the complex, and enlargement of the guest-binding cavities on the surface of the dimer (Scheme 1B and C).[15,16] Importantly, however, the complex retains its integrity in the solid state and in weakly associating solvents, even in the presence of nucleophilic halide and nitrate ions.[15] This study has shown that this unusually consistent behaviour in the $[ZnCl(Hpz^R)_3]^+$ system is only observed when R = *t*Bu.

The different stabilities of the chloride adducts $[ZnCl(Hpz^R)_3]Cl$ with different 'R' substituents may relate to the basic pK_as of the different Hpz^R ligands used:

$$Hpz^{tBu}\ (pK_a = 3.3)^{27} \geq Hpz^{Cy} > Hpz^{Ph}\ (2.1)^{27} \geq Hpz^{Tn}$$

The positioning of Hpz^{Cy} and Hpz^{Tn} on the list are inferred from the inductive properties of their 'R' groups, since pK_a measurements for these pyrazoles are not available. It is reasonable that the more basic pyrazoles, which form stronger Zn–N bonds, should be more resistant to being nucleophilically displaced by the chloride guest, as observed. Alternatively, consideration of the degree of steric protection afforded by the pyrazole 'R' substituents leads to the same ordering. In either case, the stabilities of the different $[ZnCl(Hpz^R)_3]Cl$ products to recrystallisation from chlorinated solvents perfectly follows the above trend (indefinitely stable when R = *t*Bu, partial decomposition for R = Cy, complete decomposition when R = Ph while the compound could not be made for R = Tn). The ES mass spectra and ^{13}C NMR spectra of the compounds are also broadly in agreement with these observations.

The steric influence of the pyrazole 'R' substituents is apparent in the nitrate adducts $[ZnCl(Hpz^R)_3]NO_3$ (R = *t*Bu[15] and Cy) and $[ZnBr(Hpz^{Cy})_3]NO_3$ (ESI†). The *tert*-butyl groups in $[ZnCl(Hpz^{tBu})_3]^+$ are effectively cone-shaped, and

form a consistent binding pocket that can only accommodate one anion guest. The same substituents are also large enough to prevent dimerisation of $[ZnCl(Hpz^{tBu})_3]^+$ centres through their cavities, so that all complexes of this host with smaller anions adopt the mononuclear structure (Scheme 1A) in the solid state.[14,15] In contrast, the disc-shaped cyclohexyl substituents in $[ZnY(Hpz^{Cy})_3]^+$ (Y^- = Cl^- or Br^-) are conformationally flexible, and the crystal structures show there is apparently free rotation about the *ipso*-C{pyrazole}–C{cyclohexyl} bond when the guest-binding cavity is occupied. This allows the $[ZnY(Hpz^{Cy})_3]^+$ host to interact with two guest species, either two nitrate ions or a nitrate and a water molecule (ESI†).

In conclusion, any future anion host based on the $[LM(Hpz^R)_3]^+$ design, containing a tetrahedral metal fragment, may require *tert*-butyl or similarly large pyrazole substituents to afford clean 1 : 1 host–guest chemistry (Scheme 1A).

Experimental

3{5}-Cyclohexylpyrazole,[28] 3{5}-phenylpyrazole[29] and 3{5}-(thien-2-yl)pyrazole[30] were prepared by the literature procedures, while other reagents and metal salts were purchased commercially and used as supplied. All manipulations were carried out in air using as-supplied AR grade solvents.

Synthesis of the complexes

$[ZnCl(Hpz^{Ph})_3]Cl$ and $[ZnCl_2(Hpz^{Ph})_2]$. A mixture of $ZnCl_2$ (0.16 g, 1.2 mmol) and 3{5}-phenylpyrazole (0.50 g, 3.5 mmol) in methanol (50 cm^3) was stirred at room temperature for 1 h, filtered and then evaporated to dryness. The oily residue was extracted into a minimum volume of dichloromethane and filtered. Addition of a large excess of pentane, and storage at −20 °C, afforded colourless needles of $[ZnCl(Hpz^{Ph})_3]Cl$. Recrystallisation of this compound from chloroform–diethyl ether instead yielded crystalline $[ZnCl_2(Hpz^{Ph})_2]\cdot CHCl_3$, which loses its lattice solvent upon drying *in vacuo*.

For $[ZnCl(Hpz^{Ph})_3]Cl$: found C, 57.2; H, 4.2; N, 14.9%. Calcd for $C_{27}H_{24}Cl_2N_6Zn$ C, 57.0; H, 4.3; N, 14.8%. Electrospray mass spectrum: m/z = 145 $[H_2pz^{Ph}]^+$, 352 $[^{64}Zn(Hpz^{Ph})_2]^+$. ^1H NMR spectrum ($CDCl_3$): δ 6.62 (d, 2.0 Hz, 3H, Pz H^4), 7.47 (m, 9H, Ph $H^{3\text{-}5}$), 7.69 (d, 7.5 Hz, 6H, Ph $H^{2/6}$), 7.96 (d, 2.0 Hz, 3H, Pz H^3), 13.0 (br, 3H, Pz N*H*). ^{13}C NMR spectrum ($CDCl_3$): δ 104.5 (3C, Pz C^4), 127.3 (3C, Ph C^4), 127.8 (6C, Ph $C^{3/5}$), 128.7 (6C, Ph $C^{2/6}$), 129.6 (3C, Ph C^1), 141 (v br, 3C, Pz C^3). No peak for Pz C^5 was observed. IR (nujol): 3248m, 3174w, 3140w, 1610w, 1584w, 1569m, 1479s, 1351m, 1318w, 1304m, 1266m, 1213w, 1171w, 1132s, 1092s, 1031w, 969s, 946m, 923w, 915m, 896w, 847w, 807s, 802s, 765s, 703m, 692s, 673s, 611w cm^{-1}.

For $[ZnCl_2(Hpz^{Ph})_2]$: found C, 50.9; H, 3.8; N, 13.3%. Calcd for $C_{18}H_{16}Cl_2N_4Zn$ C, 50.9; H, 3.8; N, 13.2%. Electrospray mass spectrum: m/z = 145 $[H_2pz^{Ph}]^+$, 352 $[^{64}Zn(Hpz^{Ph})_2]^+$, 392 $[^{64}Zn(pz^{Ph})(Hpz^{Ph})(NCCH_3)]^+$. ^1H NMR spectrum ($CDCl_3$): δ 6.71 (d, 2.1 Hz, 3H, Pz H^4), 7.48 (m, 9H, Ph $H^{3\text{-}5}$), 7.87 (d, 7.4 Hz, 6H, Ph $H^{2/6}$), 8.11 (d, 2.1 Hz, 3H, Pz H^3), 14.4 (br, 3H, Pz N*H*). ^{13}C NMR spectrum ($CDCl_3$): δ 103.8 (3C, Pz C^4), 126.6 (6C, Ph $C^{3/5}$), 127.9 (3C, Ph C^1), 129.7 (6C, Ph $C^{2/6}$), 130.2 (3C, Ph C^4), 142 (v br, 3C, Pz C^3), 146 (v br, 3C, Pz C^5). IR (nujol): 3141m, 3094w, 3061w, 1611w, 1588m, 1569m, 1483s, 1349m, 1316w, 1309m, 1271m, 1159w, 1133s, 1093s, 1030w, 964s, 944m, 916m, 896w, 837w, 812s, 801s, 763s, 693s, 683s, 672s, 635w cm^{-1}.

$[ZnCl(Hpz^{Cy})_3]Cl\cdot H_2O$ and $[ZnCl_2(Hpz^{Cy})_2]$. Method as above, using 3{5}-cyclohexylpyrazole (0.54 g, 3.5 mmol). Crystallisation of the crude residue from dichloromethane–pentane afforded white microcrystals of $[ZnCl(Hpz^{Cy})_3]Cl\cdot H_2O$. Recrystallisation of this material from chloroform–diethyl ether afforded the same white microcrystals, contaminated by colourless single crystals of $[ZnCl_2(Hpz^{Cy})_2]$. A small amount of the latter compound was isolated by a Pasteur separation for microanalysis.

For $[ZnCl(Hpz^{Cy})_3]Cl\cdot H_2O$: found C, 53.5; H, 7.0; N, 14.0%. Calcd for $C_{27}H_{42}Cl_2N_6Zn\cdot H_2O$ C, 53.6; H, 7.3; N, 13.9%. Electrospray mass spectrum: m/z = 151 $[H_2pz^{Cy}]^+$, 549 $[^{64}Zn^{35}Cl(Hpz^{Cy})_3]^+$, 559 $[^{64}Zn(O_2CH)(Hpz^{tBu})_3]^+$. ^1H NMR spectrum ($CDCl_3$): δ 1.2–2.0 (m, 30H, Cy $H^{2\text{-}6}$), 2.78 (m, 3H, Cy H^1), 6.20 (d, 2.0 Hz, 3H, Pz H^4), 7.91 (d, 2.0 Hz, 3H, Pz H^3), 13.4 (br, 3H, Pz N*H*). ^{13}C NMR spectrum ($CDCl_3$): δ 26.0 (3C, Cy C^4), 26.2 (6C, Cy $C^{3/5}$), 32.7 (6C, Cy $C^{2/6}$), 35.4 (3C, Cy C^1), 103.8 (3C, Pz C^4), 141.2 (3C, Pz C^3), 152.5 (3C, Pz C^5). IR (nujol): 3154w, 3131w, 3059m, 1570m, 1485s, 1340w, 1315m, 1282m, 1237w, 1221w, 1182w, 1136m, 1111m, 1057w, 1033w, 983m, 956s, 908w, 893m, 855w, 823s, 808m, 795m, 754w, 639w cm^{-1}.

For $[ZnCl_2(Hpz^{Cy})_2]$: found C, 49.4; H, 6.5; N, 12.8%. Calcd for $C_{18}H_{28}Cl_2N_4Zn$ C, 49.5; H, 6.5; N, 12.8%.

$[ZnCl_2(Hpz^{Tn})_2]$. Method as above, using 3{5}-(thien-2-yl)-pyrazole (0.53g, 3.5 mmol). Crystallisation of the crude residue from dichloromethane–pentane afforded colourless crystals of the product in analytical purity. Yield 0.34 g, 64%. Found C, 38.7; H, 2.7; N, 13.0%. Calcd for $C_{14}H_{12}Cl_2N_4S_2Zn$ C, 38.5; H, 2.8; N, 12.8%. Electrospray mass spectrum: m/z = 151 $[H_2pz^{Tn}]^+$, 364 $[^{64}Zn(Hpz^{Tn})_2]^+$. ^1H NMR spectrum ($CDCl_3$): δ 6.52 (d, 2.2 Hz, 3H, Pz H^4), 7.12 (dd, 3.7 and 5.0 Hz, 3H, Tn H^4), 7.42 (d, 5.0 Hz, 3H, Tn H^3), 7.55 (d, 3.7 Hz, 3H, Tn H^5), 7.89 (d, 2.2 Hz, 3H, Pz H^3), 12.9 (br, 3H, Pz N*H*). ^{13}C NMR spectrum ($CDCl_3$): δ 104.7 (3C, Pz C^4), 127.3, 127.8, 128.7 (all 3C, Tn C^3-C^5). No peaks for Pz C^3 and C^5 and Tn $C1$ were observed. IR (nujol): 3186m, 1797m, 1733w, 1663w, 1592s, 1508m, 1419s, 1300s, 1229m, 1171m, 1119s, 1090m, 1073s, 1043m, 960s, 900m, 850s, 837m, 808s, 794m, 777m, 705s, 667m, 643w, 603m cm^{-1}.

$[ZnBr(Hpz^{Cy})_3]Br$. A solution of $ZnBr_2$ (0.27 g, 1.2 mmol) and 3{5}-cyclohexylpyrazole (0.54 g, 3.5 mmol) in MeOH (50 cm^3) was stirred at room temperature for 1 h, then filtered and evaporated to dryness as before. Crystallisation of the residue from chloroform–pentane gave large colourless crystals of the compound that proved to suffer from twinning. Yield 0.53 g, 66%. Found C, 48.1; H, 6.3; N, 12.5%. Calcd for $C_{27}H_{42}Br_2N_6Zn$ C, 48.0; H, 6.3; N, 12.4%. Electrospray mass spectrum: m/z = 151 $[H_2pz^{Cy}]^+$, 363 $[^{64}Zn(pz^{tBu})(Hpz^{Cy})]^+$, 409 $[^{64}Zn(O_2CH)(Hpz^{Cy})_2]^+$, 593 $[^{64}Zn^{79}Br(Hpz^{Cy})_3]^+$. ^1H NMR spectrum ($CDCl_3$): δ 1.2–2.0 (m, 30H, Cy $H^{2\text{-}6}$), 2.80 (m, 3H, Cy H^1), 6.21 (d, 2.1 Hz, 3H, Pz H^4), 8.01 (d, 2.1 Hz,

3H, Pz H^3), 11.9 (v br, 3H, Pz NH). ^{13}C NMR spectrum ($CDCl_3$): δ 26.1 (3C, Cy C^4), 26.3 (6C, Cy $C^{3/5}$), 32.9 (6C, Cy $C^{2/6}$), 35.6 (3C, Cy C^1), 103.4 (3C, Pz C^4), 141.7 (3C, Pz C^3), 153.0 (3C, Pz C^5). IR (nujol): 3152w, 3130w, 3061m, 1570m, 1485s, 1312m, 1279m, 1221w, 1181w, 1136m, 1108m, 1056w, 1034w, 984m, 955s, 909w, 894m, 855w, 817s, 795s, 758m, 635m cm^{-1}.

[ZnCl(Hpz^{Ph})$_3$]BF$_4$. A mixture of $ZnCl_2$ (0.16 g, 1.2 mmol) and $AgBF_4$ (0.23 g, 1.2 mmol) was stirred in methanol (50 cm^3) for 1 h, then filtered. 3{5}-Phenylpyrazole (0.50 g, 3.5 mmol) was then added, and the mixture stirred until the solid had dissolved. Filtration and evaporation of the solution gave an oily residue that was extracted into a minimum volume of dichloromethane and filtered. Addition of a large excess of pentane, and storage at −20 °C, afforded colourless needles. Yield 0.23 g, 31%. Found C, 52.6; H, 3.9; N, 13.9%. Calcd for $C_{27}H_{24}BClF_4N_6Zn$ C, 52.3; H, 3.9; N, 13.6%. Electrospray mass spectrum: m/z = 145 [H$_2$pz^{Ph}]$^+$, 352 [^{64}Zn(Hpz^{Ph})$_2$]$^+$, 387 [^{64}Zn^{35}Cl(Hpz^{Ph})$_2$]$^+$. ^{1}H NMR spectrum ($CDCl_3$): δ 6.69 (d, 2.2 Hz, 3H, Pz H^4), 7.30 (m, 9H, Ph $H^{3\text{-}5}$), 7.70 (dd, 2.4 and 7.8 Hz, 6H, Ph $H^{2/6}$), 8.11 (d, 2.2 Hz, 3H, Pz H^3). No pyrazole NH peak was observed. ^{13}C NMR spectrum ($CDCl_3$): δ 104.3 (3C, Pz C^4), 126.5 (6C, Ph $C^{3/5}$), 127.9 (3C, Ph C^1), 129.7 (6C, Ph $C^{2/6}$), 130.3 (3C, Ph C^4). No peaks for Pz C^3 and C^5 were observed. IR (nujol): 3322m, 3145w, 1611w, 1587w, 1569m, 1481s, 1351m, 1302m, 1272m, 1132s, 1097, 1060vs, 963s, 944m, 916m, 893w, 839w, 802s, 762s, 691m, 682m, 667w, 655w cm^{-1}.

[ZnCl(Hpz^{Cy})$_3$]X (X$^-$ = NO$_3^-$, ClO$_4^-$, CF$_3$SO$_3^-$ or $\frac{1}{2}$SO$_4^{2-}$). The syntheses of all of these complexes followed the same basic procedure, as described here for the nitrate salt. A mixture of $ZnCl_2$ (0.16 g, 1.2 mmol) and $AgNO_3$ (0.20 g, 1.2 mmol) was stirred in methanol (50 cm^3) for 1 h, then filtered. 3{5}-Cyclohexylpyrazole (0.54 g, 3.5 mmol) was then added, and the mixture stirred for 30 min. Filtration and evaporation of the solution gave an oily residue that was extracted into a minimum volume of dichloromethane and filtered. Addition of a large excess of pentane, and storage at −20 °C, afforded colourless microcrystals. Analogous procedures using $AgClO_4$ (0.25 g, 1.2 mmol), $AgCF_3SO_3$ (0.31 g, 1.2 mmol) and Ag_2SO_4 (0.17 g, 0.6 mmol) afforded the corresponding salts of these anions. If necessary, the products were recrystallised from chloroform–diethyl ether. Final crystalline yields were *ca.* 55%.

For [ZnCl(Hpz^{Cy})$_3$]NO$_3$: found C, 52.6; H, 6.7; N, 15.4%. Calcd for $C_{27}H_{42}ClN_7O_3Zn$ C, 52.9; H 6.9; N 16.0%. Electrospray mass spectrum: m/z = 151 [H$_2$pz^{Cy}]$^+$, 409 [^{64}Zn(O$_2$CH)(Hpz^{Cy})$_2$]$^+$, 549 [^{64}Zn^{35}Cl(Hpz^{Cy})$_3$]$^+$, 559 [^{64}Zn(O$_2$CH)(Hpz^{Cy})$_3$]$^+$. ^{1}H NMR spectrum ($CDCl_3$): δ 1.2–2.0 (m, 30H, Cy $H^{2\text{-}6}$), 2.82 (m, 3H, Cy H^1), 6.22 (d, 2.0 Hz, 3H, Pz H^4), 7.93 (d, 2.0 Hz, 3H, Pz H^3), 12.7 (br, 3H, Pz NH). ^{13}C NMR spectrum ($CDCl_3$): δ 26.0 (3C, Cy C^4), 26.2 (6C, Cy $C^{3/5}$), 32.7 (6C, Cy $C^{2/6}$), 35.6 (3C, Cy C^1), 103.6 (3C, Pz C^4), 142 (v br, 3C, Pz C^3), 153 (v br, 3C, Pz C^5). IR (nujol): 3176m, 3137w, 3080w, 1572m, 1487s, 1309w, 1289m, 1234w, 1179w, 1153w, 1136m, 1116s, 1065w, 1031w, 985m, 958s, 893m, 854w, 831m, 797m, 752w cm^{-1}.

For [ZnCl(Hpz^{Cy})$_3$]ClO$_4$: found C, 49.9; H, 6.5; N, 13.0%. Calcd for $C_{27}H_{42}Cl_2N_6O_4Zn$ C, 49.8; H, 6.5; N, 12.9%. Electrospray mass spectrum: m/z = 151 [H$_2$pz^{Cy}]$^+$, 409 [^{64}Zn(O$_2$CH)(Hpz^{Cy})$_2$]$^+$, 549 [^{64}Zn^{35}Cl(Hpz^{Cy})$_3$]$^+$, 559 [^{64}Zn(O$_2$CH)(Hpz^{Cy})$_3$]$^+$. ^{1}H NMR spectrum ($CDCl_3$): δ 1.2–2.0 (m, 30H, Cy $H^{2\text{-}6}$), 2.81 (m, 3H, Cy H^1), 6.25 (d, 2.0 Hz, 3H, Pz H^4), 8.03 (d, 2.0 Hz, 3H, Pz H^3), 11.8 (br, 3H, Pz NH). ^{13}C NMR spectrum ($CDCl_3$): δ 26.0 (3C, Cy C^4), 26.2 (6C, Cy $C^{3/5}$), 32.7 (6C, Cy $C^{2/6}$), 35.6 (3C, Cy C^1), 103.8 (3C, Pz C^4), 142.4 (br, 3C, Pz C^3), 153.6 (br, 3C, Pz C^5). IR (nujol): 3244m, 3140w, 3114w, 1569m, 1490s, 1351w, 1309m, 1278m, 1228w, 1180w, 1120vs, 1108m, 1067m, 1049m, 1030w, 986m, 961s, 931w, 893w, 857w, 825m, 796s, 752w, 620m cm^{-1}.

For [ZnCl(Hpz^{Cy})$_3$]CF$_3$SO$_3$: found C, 47.3; H, 5.9; N, 11.9%. Calcd for $C_{28}H_{42}ClF_3N_6O_3SZn$ C, 48.0; H, 6.0; N, 12.0%. Electrospray mass spectrum: m/z = 151 [H$_2$pz^{Cy}]$^+$, 549 [^{64}Zn^{35}Cl(Hpz^{Cy})$_3$]$^+$, 559 [^{64}Zn(O$_2$CH)(Hpz^{Cy})$_3$]$^+$. ^{1}H NMR spectrum ($CDCl_3$): δ 1.2–2.0 (m, 30H, Cy $H^{2\text{-}6}$), 2.81 (m, 3H, Cy H^1), 6.21 (d, 2.0 Hz, 3H, Pz H^4), 7.97 (d, 2.0 Hz, 3H, Pz H^3), 12.1 (br, 3H, Pz NH). ^{13}C NMR spectrum ($CDCl_3$): δ 26.0 (3C, Cy C^4), 26.2 (6C, Cy $C^{3/5}$), 32.8 (6C, Cy $C^{2/6}$), 35.5 (3C, Cy C^1), 103.7 (3C, Pz C^4), 142.1 (br, 3C, Pz C^3), 154 (v br, 3C, Pz C^5). IR (nujol): 3238m, 3135w, 3108w, 1571m, 1487m, 1301m, 1277w, 1233m, 1167m, 1133w, 1113m, 1030s, 986m, 960m, 893w, 854w, 800m, 769w, 637m cm^{-1}.

For [ZnCl(Hpz^{Cy})$_3$]$_2$SO$_4$: found C, 53.8; H, 7.0; N, 14.0%. Calcd for $C_{54}H_{84}Cl_2N_{12}O_4SZn_2$ C, 54.1; H, 7.1; N, 14.0%. Electrospray mass spectrum: m/z = 151 [H$_2$pz^{Cy}]$^+$, 399 [^{64}ZnCl(Hpz^{Cy})$_2$]$^+$, 549 [^{64}Zn^{35}Cl(Hpz^{Cy})$_3$]$^+$, 683 [^{64}Zn$_2$^{35}Cl$_3$(Hpz^{Cy})$_3$]$^+$. ^{1}H NMR spectrum ($CDCl_3$): δ 1.2–2.0 (m, 30H, Cy $H^{2\text{-}6}$), 2.81 (m, 3H, Cy H^1), 6.19 (d, 2.0 Hz, 3H, Pz H^4), 7.93 (d, 2.0 Hz, 3H, Pz H^3), 13.6 (br, 3H, Pz NH). ^{13}C NMR spectrum ($CDCl_3$): δ 26.1 (3C, Cy C^4), 26.3 (6C, Cy $C^{3/5}$), 32.8 (6C, Cy $C^{2/6}$), 35.6 (3C, Cy C^1), 103.2 (3C, Pz C^4). No peaks for Pz C^3 and C^5 were observed. IR (nujol): 3153w, 3130w, 1569m, 1485m, 1339w, 1314m, 1280m, 1221w, 1181w, 1136n, 1111s, 1057w, 1032m, 983m, 955s, 908w, 893m, 854w, 820m, 795m, 752w, 640m cm^{-1}.

[ZnBr(Hpz^{Cy})$_3$]NO$_3$·H$_2$O. Method as above, using $ZnBr_2$ (0.27 g, 1.2 mmol) and $AgNO_3$ (0.20 g, 1.2 mmol). Slow diffusion of pentane vapour into a chloroform solution of the crude residue yielded single crystals of the product. Yield 0.38 g, 47%. Found C, 48.2; H, 6.4; N, 14.5%. Calcd for $C_{27}H_{44}BrN_7O_4Zn$ C, 48.0; H, 6.6; N, 14.5%. Electrospray mass spectrum: m/z = 151 [H$_2$pz^{Cy}]$^+$, 363 [^{64}Zn(pz^{tBu})(Hpz^{Cy})]$^+$, 409 [^{64}Zn(O$_2$CH)(Hpz^{Cy})$_2$]$^+$, 559 [^{64}Zn(O$_2$CH)(Hpz^{Cy})$_3$]$^+$, 593 [^{64}Zn^{79}Br(Hpz^{Cy})$_3$]$^+$. ^{1}H NMR spectrum ($CDCl_3$): δ 1.2–2.0 (m, 30H, Cy $H^{2\text{-}6}$), 2.80 (m, 3H, Cy H^1), 6.20 (d, 2.1 Hz, 3H, Pz H^4), 7.97 (d, 2.1 Hz, 3H, Pz H^3), 11.9 (v br, 3H, Pz NH). ^{13}C NMR spectrum ($CDCl_3$): δ 26.1 (3C, Cy C^4), 26.3 (6C, Cy $C^{3/5}$), 32.7 (6C, Cy $C^{2/6}$), 35.6 (3C, Cy C^1), 103.5 (3C, Pz C^4), 142.0 (3C, Pz C^3), 153.4 (3C, Pz C^5). IR (nujol): 3186m, 3139w, 3081w, 1566m, 1487s, 1351w, 1337w, 1289m, 1226w, 1182w, 1136m, 1111s, 1060w, 1028w, 984m, 957s, 909w, 894w, 853w, 832m, 795m, 752w cm^{-1}.

Single crystal X-ray structure determinations

All diffraction data were measured using a Bruker X8 Apex diffractometer, with graphite-monochromated Mo-K_α radiation (λ = 0.71073 Å) generated by a rotating anode. The diffractometer is fitted with an Oxford Cryostream low temperature device. Experimental details of the structure determinations in this study are given in Table 4. All the structures were solved by direct methods (SHELXS97[31]), and developed by full least-squares refinement on F^2 (SHELXL97[31]). Crystallographic figures were prepared using XSEED,[32] which incorporates POVRAY.[33]

$[ZnCl_2(Hpz^{Ph})_2]\cdot CHCl_3$, $[ZnCl_2(Hpz^{Cy})_2]$, $[ZnCl(Hpz^{Ph})_3]Cl$ and $[ZnCl(Hpz^{Cy})_3]ClO_4$. No disorder was detected during refinement of these structures, and no restraints were applied. All non-H atoms were refined anisotropically, and all H atoms were placed in calculated positions and refined using a riding model.

$[ZnCl_2(Hpz^{Tn})_2]$. There are two molecules in the asymmetric unit, labelled 'A' and 'B', that are associated into a unique dimer by N–H···Cl hydrogen bonding. Two of the four unique thienyl groups in the model are disordered over two sites: C(9A)–C(13A) (refined occupancy 0.73) and C(9A), S(10C)–C(13C) (0.27); and, C(9B)–C(13B) (0.80) and C(9B), S(10D)–C(13D) (0.20) so the *ipso* C atoms C(9A) and C(9B) are wholly occupied and shared between both disorder sites. The following restraints were applied to these residues: C–S = 1.72(2), thienyl *C*2–*C*3 = *C*4–*C*5 = 1.36(2) and thienyl *C*3–*C*4 = 1.42(2) Å. All non-H atoms with occupancy > 0.5 were refined anisotropically, while all H atoms were placed in calculated positions and refined using a riding model.

$[ZnCl(Hpz^{Cy})_3]NO_3$. Two of the three cyclohexyl substituents in the complex are disordered, both over two sites, labelled 'A' and 'B': C(19)–C(24) (refined A : B occupancies 0.61 : 0.39) and C(30)–C(35) (0.50 : 0.50). All disordered C–C bonds were restrained to 1.52(2) Å, and non-bonded 1,3-C···C contacts within each partial residue to 2.48(2) Å. The disorder sites C(19A)–C(24A) and C(30A^{vi})–C(35A^{vi}) (symmetry code (vi): 1 − *x*, −*y*, −*z*) probably cannot be simultaneously occupied in the centrosymmetric dimer, owing to a steric contact C(23A)···C(32A^{vi}) = 3.33 Å. All crystallographically ordered non-H atoms were refined anisotropically, while all H atoms were placed in calculated positions and refined using a riding model.

$[ZnBr(Hpz^{Cy})_3]NO_3\cdot H_2O$. The asymmetric unit contains half a molecule, with Zn(1), Br(2), N(14)–C(19), C(22), nitrate ion N(23)–O(26) and water molecule O(27) all lying on the crystallographic mirror plane *x*, ½, *z*. No disorder was detected during refinement. All non-H atoms were refined anisotropically, while H atoms were placed in calculated positions and refined using a riding model. The positions of the H atoms in the half-water molecule O(27) could not be refined successfully, so these were also placed in calculated positions and refined with a riding model, assuming a tetrahedral disposition of H atoms and H bonds to O(27). This calculation procedure used means that the two O(27)–H bonds are artificially long, at 0.99 Å (0.85 Å would be a more meaningful value). This accounts for the apparent steric clash between H(9A) and H(27A) (which are only 2.3 Å apart in the model), and means that the metric parameters for the two hydrogen bonds for the two hydrogen bonds donated by O(27) should be treated with care.

Table 4 Experimental details for the single crystal structure determinations in this study

	$[ZnCl_2(Hpz^{Ph})_2]\cdot CHCl_3$	$[ZnCl_2(Hpz^{Tn})_2]$	$[ZnCl_2(Hpz^{Cy})_2]$	$[ZnCl(Hpz^{Ph})_3]Cl$	$[ZnCl(Hpz^{Cy})_3]NO_3$	$[ZnBr(Hpz^{Cy})_3]NO_3\cdot H_2O$	$[ZnCl(Hpz^{Cy})_3]ClO_4$
Molecular formula	$C_{19}H_{17}Cl_5N_4Zn$	$C_{14}H_{12}Cl_2N_4S_2Zn$	$C_{18}H_{28}Cl_2N_4Zn$	$C_{27}H_{24}Cl_2N_6Zn$	$C_{27}H_{42}ClN_7O_3Zn$	$C_{27}H_{44}BrN_7O_4Zn$	$C_{27}H_{42}Cl_2N_6O_4Zn$
M_r	543.99	436.67	436.71	568.79	613.50	675.97	650.94
Crystal class	Triclinic	Monoclinic	Monoclinic	Orthorhombic	Triclinic	Orthorhombic	Monoclinic
Space group	$P\bar{1}$	$P2_1/c$	$P2_1/n$	*Pbca*	$P\bar{1}$	*Pnma*	$C2/c$
a/Å	8.8197(11)	13.0349(13)	10.6333(9)	17.685(2)	11.9059(9)	11.5875(16)	24.414(3)
b/Å	12.0309(13)	20.252(2)	11.5074(11)	17.185(2)	12.3024(9)	15.191(3)	16.933(2)
c/Å	12.1267(15)	14.7727(17)	17.8610(17)	17.758(3)	12.4108(9)	18.270(3)	19.071(4)
α/°	98.231(6)	—	—	—	66.546(3)	—	—
β/°	104.297(6)	113.506(5)	97.665(5)	—	74.875(4)	—	126.019(5)
γ/°	104.816(6)	—	—	—	71.417(4)	—	—
V/Å^3	1175.8(2)	3576.1(7)	2166.0(3)	5397.0(13)	1561.8(2)	3215.9(8)	6376.6(18)
Z	2	8	4	8	2	4	8
μ (Mo-K_α)/mm^{-1}	1.626	1.908	1.389	1.135	0.910	2.048	0.979
T/K	150(2)	150(2)	150(2)	150(2)	150(2)	150(2)	150(2)
Measured reflections	16 132	31 466	37 946	124 368	55 714	110 627	113 573
Independent reflections	6145	8216	5178	6562	7719	4191	7384
R_{int}	0.034	0.065	0.027	0.061	0.039	0.054	0.108
$R(F)^a$	0.034	0.044	0.020	0.030	0.043	0.032	0.040
w$R(F^2)^b$	0.081	0.116	0.053	0.077	0.108	0.093	0.089
Goodness of fit	1.066	1.023	1.038	1.052	1.061	1.118	1.028

^{a} $R = \Sigma[|F_o| - |F_c|]/\Sigma|F_o|$. ^{b} w$R = [\Sigma w(F_o^2 - F_c^2)/\Sigma wF_o^4]^{1/2}$.

There are three residual Fourier peaks $>1.0\ e\ \text{Å}^{-3}$ in the final difference map. Two of these lie in the nitrate ion, and may indicate a weak alternative disorder site for that group. The third peak lies 1.2 Å from Br(2). The deepest Fourier hole of $-1.2\ e\ \text{Å}^{-3}$ is <0.1 Å from Zn(1).

Other measurements

Electrospray (ES) mass spectra were obtained with a Waters ZQ4000 TOF spectrometer using a MeCN feed solution. All peaks show correct isotopic distributions for their assigned molecular ions. CHN microanalyses were performed by the University of Leeds School of Chemistry microanalytical service. ^{1}H NMR spectra were run on a Bruker ARX250 spectrometer, operating at 250.1 MHz. Infrared spectra were run as nujol mulls between NaCl winows, using a Nicolet Avatar 360 spectrophotometer.

Acknowledgements

This work was funded by the EPSRC and the University of Leeds. MAH thanks the Research Centre for Materials Science, Nagoya University, for a sabbatical that allowed the writing of this paper.

Notes and references

1 P. D. Beer and P. A. Gale, *Angew. Chem., Int. Ed.*, 2001, **40**, 486; K. Bowman-James, *Acc. Chem. Res.*, 2005, **38**, 671.
2 *Anion Sensing*, *Top. Curr. Chem.*, ed. I. Stibor, 2005, p. 255.
3 P. A. Gale, 35 Years of Synthetic Anion Receptor Chemistry, *Coord. Chem. Rev.*, 2003, **240**.
4 P. A. Gale, Anion Coordination Chemistry II, *Coord. Chem. Rev.*, 2006, **250**(23–24).
5 *Recognition of Anions*, *Structure and Bonding*, ed. R. Vilar, Springer-Verlang, Berlin, 2008, vol. 129.
6 A. P. Davis, D. N. Sheppard and B. D. Smith, *Chem. Soc. Rev.*, 2007, **36**, 348.
7 E. A. Katayev, G. V. Kolesnikov and J. L. Sessler, *Chem. Soc. Rev.*, 2009, **38**, 1572.
8 P. D. Beer, *Acc. Chem. Res.*, 1998, **31**, 71; P. D. Beer and E. J. Hayes, *Coord. Chem. Rev.*, 2003, **240**, 167; V. Amendola and L. Fabbrizzi, *Chem. Commun.*, 2009, 513; J. W. Steed, *Chem. Soc. Rev.*, 2009, **38**, 506.
9 J. Pérez and L. Riera, *Chem. Commun.*, 2008, 533; J. Pérez and L. Riera, *Chem. Soc. Rev.*, 2008, **37**, 2658.
10 V. Amendola, L. Fabbrizzi, C. Mangano, P. Pallavicini, A. Poggi and A. Taglietti, *Coord. Chem. Rev.*, 2001, **219–221**, 821; V. McKee, J. Nelson and R. M. Town, *Chem. Soc. Rev.*, 2003, **32**, 309.
11 P. A. Tasker, C. C. Tong and A. N. Westra, *Coord. Chem. Rev.*, 2007, **251**, 1868.
12 A. Looney, G. Parkin and A. L. Rheingold, *Inorg. Chem.*, 1991, **30**, 3099.
13 D. L. Reger, Y. Ding, A. L. Rheingold and R. L. Ostrander, *Inorg. Chem.*, 1994, **33**, 4226.
14 X. Liu, C. A. Kilner and M. A. Halcrow, *Chem. Commun.*, 2002, 704.
15 S. L. Renard, C. A. Kilner, J. Fisher and M. A. Halcrow, *J. Chem. Soc., Dalton Trans.*, 2002, 4206.
16 S. L. Renard, A. Franken, C. A. Kilner, J. D. Kennedy and M. A. Halcrow, *New J. Chem.*, 2002, **26**, 1634.
17 M. Onishi, M. Yamaguchi, S. Kumagae, H. Kawano and Y. Arikawa, *Inorg. Chim. Acta*, 2006, **359**, 990.
18 S. Nieto, J. Pérez, V. Riera, D. Miguel and C. Alvarez, *Chem. Commun.*, 2005, 546; S. Nieto, J. Pérez, L. Riera, V. Riera and D. Miguel, *Chem.–Eur. J.*, 2006, **12**, 2244.
19 S. Nieto, J. Pérez, L. Riera, V. Riera, D. Miguel, J. A. Golen and A. L. Rheingold, *Inorg. Chem.*, 2007, **46**, 3407.
20 M. Arroyo, D. Miguel, F. Villafañe, S. Nieto, J. Pérez and L. Riera, *Inorg. Chem.*, 2006, **45**, 7018; J. Pérez, L. Riera, L. Ion, V. Riera, K. M. Anderson, J. W. Steed and D. Miguel, *Dalton Trans.*, 2008, 878.
21 V. Amendola, D. Esteban-Gómez, L. Fabbrizzi and M. Licchelli, *Acc. Chem. Res.*, 2006, **39**, 343.
22 L. Pauling, *The Nature of the Chemical Bond*, Cornell University Press, Ithaca, NY, 3rd edn, 1960, pp. 257–264.
23 E. Bouwman, W. L. Driessen, R. A. G. de Graaff and J. Reedijk, *Acta Crystallogr., Sect. C: Cryst. Struct. Commun.*, 1984, **40**, 1562; P. D. Verweij, F. J. Rietmeijer, R. A. G. De Graaff, A. Erdonmez and J. Reedijk, *Inorg. Chim. Acta*, 1989, **163**, 223; E. Libertini, K. Yoon and G. Parkin, *Polyhedron*, 1993, **12**, 2539; G. Hanggi, H. Schmalle and E. Dubler, *Inorg. Chem.*, 1993, **32**, 6095; Z. K. Jacimovic, B. V. Prelesnik, G. A. Bogdanovic, E. Z. Iveges and V. M. Leovac, *Z. Kristallogr. - New Cryst. Struct.*, 1998, **213**, 35; E. Cavero, S. Uriel, P. Romero, J. L. Serrano and R. Giménez, *J. Am. Chem. Soc.*, 2007, **129**, 11608; S. Bergner, G. Wolmershäuser, H. Kelm and W. R. Thiel, *Inorg. Chim. Acta*, 2008, **361**, 2059.
24 S. Bieller, A. Haghiri, M. Bolte, J. W. Bats, M. Wagner and H.-W. Lerner, *Inorg. Chim. Acta*, 2006, **359**, 1559.
25 D. M. P. Mingos and A. L. Rohl, *J. Chem. Soc., Dalton Trans.*, 1991, 3419.
26 R. M. Claramunt, C. López, M. D. Santa Maria, D. Sanz and J. Elguero, *Prog. Nucl. Magn. Reson. Spectrosc.*, 2006, **49**, 169.
27 J. Elguero, E. Gonzalez and R. Jacquier, *Bull. Soc. Chim. Fr.*, 1968, 5009.
28 S. Trofimenko, A. L. Rheingold and L. M. Liable Sands, *Inorg. Chem.*, 2002, **41**, 1889.
29 S. Trofimenko, J. C. Calabrese and J. S. Thompson, *Inorg. Chem.*, 1987, **26**, 1507.
30 J. C. Calabrese, P. J. Domaille, S. Trofimenko and G. J. Long, *Inorg. Chem.*, 1991, **30**, 2795.
31 G. M. Sheldrick, *Acta Crystallogr., Sect. A: Found. Crystallogr.*, 2008, **64**, 112.
32 L. J. Barbour, *J. Supramol. Chem.*, 2001, **1**, 189.
33 *POVRAY v. 3.5*, Persistence of Vision Raytracer Pty. Ltd., Williamstown, Victoria, Australia, 2002, http://www.povray.org.

